

Huaxiong Huang

*Department of Mathematics and Statistics
York University
Toronto, Ontario
Canada M3J 1P3
hhuang@yorku.ca*

Studiegroep wiskunde met de industrie

Non-Newtonian effects on ink-jet droplet formation

Study groups with industry are meetings where people from industry meet mathematicians to tackle industrial problems. The first such meeting was held in the sixties at the University of Oxford. Nowadays study groups take place all over the world. The 45th European Study Group with Industry took place in February 2003 at the Lorentz Center of Leiden University.

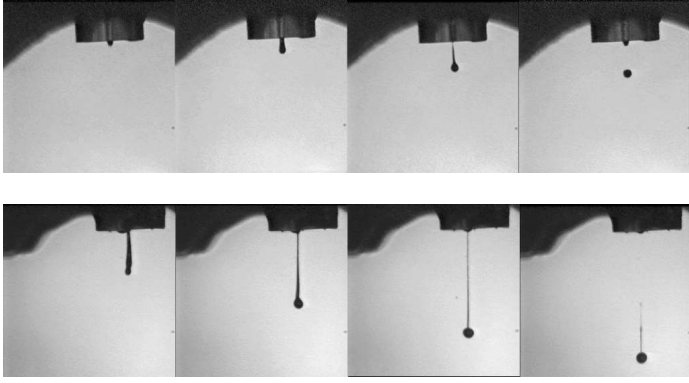
One of the problems for the study group was brought in by Philips. This company is trying to adapt ink-jet technology to print light-emitting polymer displays. The polymers involved show visco-elastic behaviour very different from normal inks. The question posed to the study group was to model the visco-elastic behaviour of the jetted polymer solution to obtain information about the droplet formation of the polymer liquid.

Light-emitting polymer display (LED) is a new technology. LED devices do not have viewing angle restriction, which gives them a major advantage over the existing liquid crystal displays (LCDs). The active material in the display is a very thin semi-conducting polymer layer of order 100 nanometer. To obtain these thin layers a small concentration of the polymer is dissolved in a suitable solvent. Different colours can be obtained with different polymers. To make a full colour display, red, green and blue polymer solutions have to be applied in pixels of typically 66×200 micron. The method with which the polymer solutions are applied is by means of ink-jet printing. Individual droplets are printed in the pixels and by evaporating the solvent the final polymer layer is obtained. The polymers have high molecular weights which cause the droplet formation to be quite different from an ordinary Newtonian liquid; that is, a long filament may form. This can give rise to a decrease in the placement accuracy of the droplets on the

substrate. Therefore, when predicting the behaviour of a droplet in an ink-jet printer the material parameters of the liquid are very important.

The viscosity of an ink is an important parameter for the droplet formation in an ink-jet head. Standard in the ink-jet printing world is to measure the shear viscosity of the liquid. Most common inks are Newtonian liquids and the shear viscosity is a suitable characterization parameter. For inks that are solutions of a high molecular weight polymer in small concentrations in a solvent, the situation is quite different. It has been observed in the laboratory that the droplet formation of these solutions is considerably different from the predictions based on the shear viscosity alone, where it is assumed that the solution is a pure Newtonian liquid. For example, more energy is needed to eject the droplet and some droplets are formed with a filament, which can break up into satellite droplets. When these solutions are measured in a shear rheometer, the viscosity is shown to be a constant and is in the proper regime for ink-jet printing. This suggests that the filament formation during the ink-jet printing is caused by the different behaviour in the elongational viscosity. This is not surprising since it is well known (see for example [11] and references therein) that a small concentration of a high molecular weight polymer in a solvent can increase the elongational viscosity substantially.

Since the shear viscosity cannot be used to characterize the inks, we need to obtain the elongational viscosity in order to make reasonable predictions. The problem is that the elongational viscosity is not easy to measure, especially in the range of deformation rate of ink-jet printing, in contrast to the shear viscosity. On the other hand, the experimental results indicate that the tail behaviour is strongly affected by the properties of the polymer. This



photographs: courtesy P. C. Duineveld, Philips Research

Figure 1 Above: a simple experiment of the filament formation of an ink-jet printed droplet, here the filament formation is modest. Below: the same experiment as above, but now the filament formation is extreme.

suggests that if a mathematical model of the non-Newtonian fluid can be constructed, then the model can be calibrated using the tail-length or other information of the droplets by varying the operational conditions. This approach can be viewed as an indirect means to obtain information on the elongational viscosity. Obviously, the same model can also be used to study the dynamic process of droplet formation. In this article, we describe some preliminary results based on a one-dimensional model for the elongational viscosity and for the dynamics of droplet formation.

Mathematical Model

The problem of droplet formation consists of two stages: the ejection of liquid from the nozzle and the breakup liquid filament. For an ink-jet printer, this is achieved using a large number of miniature valveless pumps. The pumps are actuated electronically, by locally heating elements of the liquid to high temperatures. Vapor bubbles are created and grow explosively at desirable locations inside pumps. As a result, they push a small amount of liquid at high velocity through nozzles. To completely understand the formation of an ink-jet droplet, detailed two (possibly three) dimensional hydrodynamics models are needed. However, the exit flow of general non-Newtonian fluid is still far from being understood and simple models are used instead. For example, the process has been investigated using an energy argument while the behaviour of the pumps is modeled as a Helmholtz resonator in [5]. Since our main purpose is to study the non-Newtonian effects on the filament (tail) of the droplet, we will not investigate the exit flow in detail. Instead, we will follow the energy argument in [5] for the formation of droplets.

The breakup of a liquid jet in the context of Newtonian fluid has been well-studied by several researchers based on (one-dimensional) thin jet approximation. Such models predict the breakup of jets in finite time, described by a similarity solution [7–8]. It is well-known that visco-elasticity and other non-Newtonian effects delay the breakup by suppressing surface tension [4, 9–10, 12]. Nevertheless, pinch-off may still occur due to the surface tension force, which becomes dominant when the radius of the liquid jet is small. The problem being investigated here, however, has some distinct features. The ink-jet is driven by thermal expansion of the liquid (or a piezoelectric mechanism) with a period on the order of 20 micro-seconds [5]. Therefore, the breakup of the ink-jet may be caused by the highly oscillatory nature of the flow (at least initially). Our main objective is to set up a mathemati-

cal model and investigate numerically the combined effect of the high frequency transient flow and the non-Newtonian nature of the polymer solution.

Initial droplet formation

In order to provide the initial condition for the evolution of the droplet tail, we use a simple energy argument to obtain the time t_0 when the droplet forms. The basic argument is based on energy consideration, following that of [5]. We assume that before the droplet forms, the fluid simply flows out of the nozzle as a liquid cylinder with radius R_n . At t_0 , the droplet forms and it moves with the fluid velocity at the nozzle, $V(t_0)$. Thus, we can estimate the total kinetic energy flowing out of the nozzle during the period $0 \leq t \leq t_0$ as

$$T_{k.e.} = \int_0^{t_0} \frac{1}{2} \rho A V^3 dt$$

where A is the nozzle cross section area, ρ is the fluid density and V is the fluid velocity at the nozzle exit, assumed to be given. The total kinetic energy associated with the liquid cylinder at t_0 is

$$T_{k.e.l.} = \int_0^{t_0} \frac{1}{2} \rho A V dt V^2(t_0).$$

The total surface energy associated with the liquid cylinder at t_0 is

$$T_{s.e.l.} = \sigma 2\pi R_n \int_0^{t_0} V dt$$

where σ is the surface tension coefficient between the liquid and the air. We assume that the energy dissipation due to viscosity is negligible, then the drop forms at t_0 when $T_{k.e.l.} + T_{s.e.l.}$ is about to exceed $T_{k.e.}$, i.e., the total kinetic energy is not sufficient to maintain the growth of the liquid cylinder out of the nozzle beyond t_0 .

In addition, we assume that after the droplet forms, it immediately takes a spherical shape and is connected with the nozzle by a tail, in the shape of a cylinder. The evolution and the eventual breakup of the tail is the subject of the rest of this article.

Tail evolution

The governing equations for the fluid inside the tail of the droplet are the conservation of momentum and incompressibility equations

$$\rho \left[\frac{\partial \vec{v}}{\partial t} + (\vec{v} \cdot \nabla) \vec{v} \right] = \nabla \cdot \mathbf{T} - \nabla p$$

$$\nabla \cdot \vec{v} = 0,$$

where ρ is the density, \vec{v} is the velocity, \mathbf{T} is the viscous stress tensor and p is the pressure. Here we have neglected the effect of the gravity.

To simplify the discussion, we make the following assumptions:

- i. The flow is essentially one-dimensional since the tail radius is small compared to its length L . Furthermore, in general the variation of the tail radius is also small, except during the initial stage of droplet formation and when tail breaks up (pinch-off occurs).
- ii. The formation of the initial droplet and subsequently its tail

are determined by the flow at the exit of the nozzle. We assume that the flow-rate is a periodic function of time given by

$$Q = A_n V, \quad V = V_n e^{-\beta t} \sin(\omega t)$$

where A_n is the nozzle cross section area, V is the velocity at the nozzle exit, V_n is the (un-damped) mean velocity at the nozzle, β is the damping rate due to energy dissipation of the fluid before it reaches the exit and ω is the frequency of the oscillation.

- iii. We assume that the droplet forms at t_0 with an initial tail length L_0 . The droplet is assumed to be a sphere with a fixed radius R_d .
- iv. The tail is of cylindrical shape with radius R which is both a function of time t and spatial coordinate x , measured from the nozzle. Upon exit from the nozzle, the radius R_c of the fluid volume contracts and its value is assumed to be known and equals to the tail radius.
- v. Since ω is large, and the break-up of the tail normally occurs within a short time period after the droplet forms, temperature effects on both the surface tension coefficient σ and fluid (elongational) viscosity $\hat{\mu}$ are negligible.
- vi. Finally, we assume that the fluid is incompressible with a constant density.

The governing equations for the evolution of the tail and the motion of the droplet can now be re-written as ¹

$$\begin{aligned} \frac{\partial A}{\partial t} + \frac{\partial Au}{\partial x} &= 0, \\ \rho \left(\frac{\partial Au}{\partial t} + \frac{\partial Au^2}{\partial x} \right) &= \frac{\partial}{\partial x} \left(A\tau + A \frac{\sigma}{R} \right), \end{aligned}$$

for $0 \leq x \leq L(t)$, where $A = 2\pi R^2$ is the cross section area of the tail and τ is the axial viscous stress. For Newtonian fluid, we have

$$\tau = 3\mu \frac{\partial u}{\partial x}$$

where the constant μ is the shear viscosity. For non-Newtonian fluid, the viscous stress is no longer linearly proportional to the strain rate. In this study, we use a simple model in the form

$$\begin{aligned} \tau &= \hat{\mu} \frac{\partial u}{\partial x} + kw, \\ \frac{\partial w}{\partial t} &= \frac{\partial u}{\partial x}. \end{aligned}$$

Here $\hat{\mu}$ is the elongational viscosity, w is the velocity and relative displacement of the fluid in the axial direction and k is assumed to be a constant. The governing equations now become

$$\begin{aligned} \frac{\partial A}{\partial t} + \frac{\partial Au}{\partial x} &= 0, \\ \rho \left(\frac{\partial Au}{\partial t} + \frac{\partial Au^2}{\partial x} \right) &= \frac{\partial}{\partial x} \left(A\hat{\mu} \frac{\partial u}{\partial x} + Ak \int_{t_{ref}}^t \frac{\partial u}{\partial x} dt + A \frac{\sigma}{R} \right), \end{aligned}$$

where t_{ref} is some reference time.

The boundary conditions for the above equations are normally required at $x = 0$ (exit) and $x = L$ (when the tail joins the droplet). They are

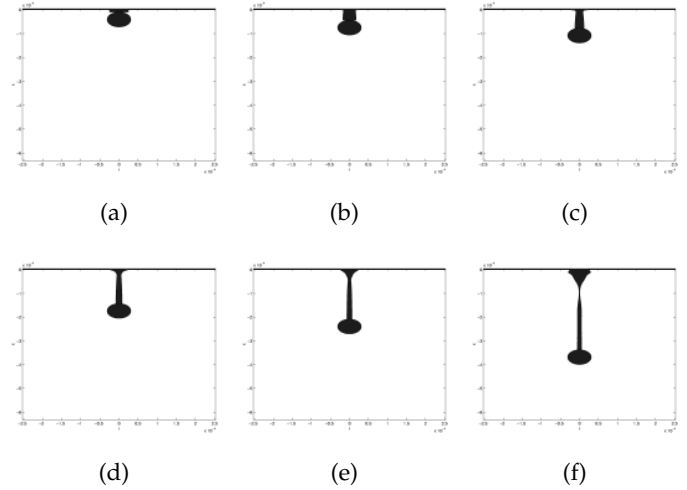


Figure 2 Case 1. Power-law elongational viscosity with $\gamma = 1.1$. Shape of the tail for $R_s = 1.25R_n$ and $R_c = R_n$ at (a) $t = 0$; (b) $t = 0.5t_0$; (c) $t = t_0$; (d) $t = 2t_0$; (e) $t = 3t_0$; (f) $t = 5t_0$.

$$\begin{aligned} x = 0 : R(0, t) &= R_c, \quad u(0, t) = \frac{Q}{2\pi R_c^2}, \\ x = L(t) : u(L(t), t) &= \frac{dL}{dt}, \quad A\hat{\mu} \frac{\partial u}{\partial x} + Ak \int_{t_{ref}}^t \frac{\partial u}{\partial x} dt + A \frac{\sigma}{R} = F. \end{aligned}$$

The motion of the droplet is given by the Newton second law of motion

$$F = -ma, \quad a = \frac{d^2L}{dt^2}.$$

We note that the boundary condition on R is not required at $x = L$ since the velocity there is positive and the characteristic goes out of the domain. However, the flow (velocity) at $x = 0$ may reverse its direction and in that case the radius should not be given at $x = 0$. When the velocity is negative, it is likely that the contact line may move inside the nozzle and the flow pattern becomes quite complicated. Therefore, the artificial boundary condition for R at $x = 0$ for negative velocity is not physical. A possible remedy will be to allow the exit boundary to move with the fluid when the velocity is negative, without considering a two-dimensional model. This issue is not considered here.

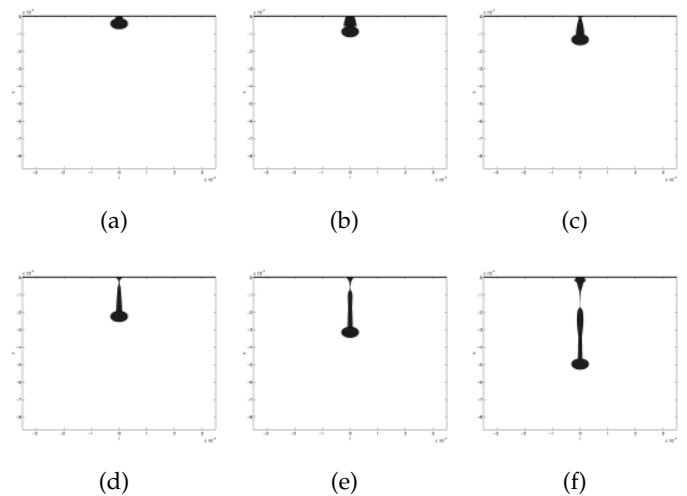


Figure 3 Case 2. Power-law elongational viscosity with $\gamma = 1.1$. Shape of the tail for $R_s = 1.25R_n$ and $R_c = 0.5R_n$ at (a) $t = 0$; (b) $t = 0.5t_0$; (c) $t = t_0$; (d) $t = 2t_0$; (e) $t = 3t_0$; (f) $t = 5t_0$.

Numerical Method

We now describe the numerical method used for solving the model equations derived earlier.

Coordinate transformation

We first define a one-dimensional map

$$\xi = \frac{x}{L(t)}, \quad t = t.$$

Under this transformation, we have

$$\frac{\partial}{\partial x} = \frac{1}{L} \frac{\partial}{\partial \xi}, \quad \frac{\partial}{\partial t} = \frac{\partial}{\partial t} - \frac{\xi \dot{L}}{L} \frac{\partial}{\partial \xi}.$$

The governing equations become

$$\begin{aligned} \frac{\partial R}{\partial t} &= \frac{\xi \dot{L} - u}{L} \frac{\partial R}{\partial \xi} - \frac{R}{2L} \frac{\partial u}{\partial \xi}, \\ \frac{\partial u}{\partial t} &= \frac{\xi \dot{L}}{L} \frac{\partial u}{\partial \xi} + \frac{1}{\rho R^2 L} \frac{\partial}{\partial \xi} \left(\frac{\hat{\mu} R^2}{L} \frac{\partial u}{\partial \xi} + k R^2 w + \sigma R \right), \\ \frac{\partial w}{\partial t} &= \frac{1}{L} \frac{\partial u}{\partial \xi}, \end{aligned}$$

where $\dot{L} = \frac{dL}{dt}$. The boundary and initial conditions are

$$\begin{aligned} = 0 : u(0, t) &= V, \quad R(0, t) = R_c, \\ = 1 : u &= \dot{L}, \quad \frac{\hat{\mu}}{L} \frac{\partial u}{\partial \xi} + k w + \frac{\sigma}{R} = -\frac{M}{\pi R^2} a, \end{aligned}$$

where $a = \frac{d^2 L}{dt^2}$ and $M = \frac{4\pi R_s^3 \rho}{3}$ are the acceleration and the mass of the droplet, respectively.

Finite difference discretisation

We set up a uniform grid $\xi_j = jh$ for $j = 0, 1, \dots, N$ with $h = 1/N$ and define $U_j(t)$ and $W_j(t)$ as approximations of $u(\xi_j, t)$ and $w(x_j, t)$. Applying the finite difference approximation in ξ and using short-hand notation for time differentiation yields

$$\begin{aligned} \dot{R}_j &= [1 + \text{sign}(\xi_j \dot{L} - U_j)] \frac{\xi_j \dot{L} - U_j}{2L} \frac{R_{j+1} - R_j}{h} \\ &\quad + [1 - \text{sign}(\xi_j \dot{L} - U_j)] \frac{\xi_j \dot{L} - U_j}{2L} \frac{R_j - R_{j-1}}{h} \\ &\quad - \frac{R_j}{2L} \frac{U_j - U_{j-1}}{h}, \\ \dot{U}_j &= [1 + \text{sign}(\dot{L})] \frac{\xi_j \dot{L}}{2L} \frac{U_{j+1} - U_j}{h} \\ &\quad + [1 - \text{sign}(\dot{L})] \frac{\xi_j \dot{L}}{2L} \frac{U_j - U_{j-1}}{h} \\ &\quad + \frac{1}{\rho R_j^2 L h} \left(\frac{\hat{\mu}_{j+1/2} R_{j+1/2}^2}{L} \frac{U_{j+1} - U_j}{h} \right. \\ &\quad + k R_{j+1/2}^2 W_{j+1/2} + \sigma R_{j+1/2} \\ &\quad \left. - \frac{\hat{\mu}_{j-1/2} R_{j-1/2}^2}{L} \frac{U_j - U_{j-1}}{h} \right. \\ &\quad \left. - k R_{j-1/2}^2 W_{j-1/2} - \sigma R_{j-1/2} \right), \\ \dot{W}_{j+1/2} &= \frac{1}{L} \frac{U_{j+1} - U_j}{h}, \quad \dot{W}_{j-1/2} = \frac{1}{L} \frac{U_j - U_{j-1}}{h}, \end{aligned}$$

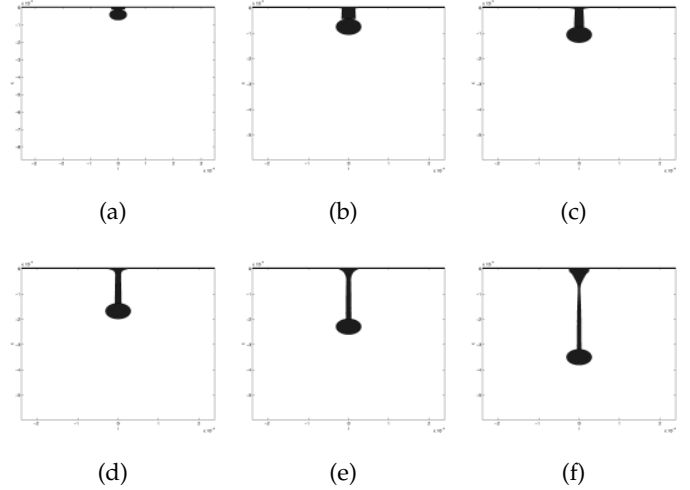


Figure 4 Case 3. Power-law elongational viscosity with $\gamma = 1.5$. Shape of the tail for $R_s = 1.25R_n$ and $R_c = R_n$ at (a) $t = 0$; (b) $t = 0.5t_0$; (c) $t = t_0$; (d) $t = 2t_0$; (e) $t = 3t_0$; (f) $t = 5t_0$.

where

$$\begin{aligned} \hat{\mu}_{j+1/2} &= \hat{\mu} \left(\frac{U_{j+1} - U_j}{Lh} \right), \\ \hat{\mu}_{j-1/2} &= \hat{\mu} \left(\frac{U_j - U_{j-1}}{Lh} \right), \\ R_{j\pm 1/2} &= \frac{1}{2} (R_j + R_{j\pm 1}) \end{aligned}$$

for $j = 1, \dots, N-1$. Note that the upwind scheme is used for the convective terms in both continuity and momentum equations.

At the boundary, we have

$$\dot{U}_0 = V_n e^{-\beta t} [\omega \cos(\omega t) - \beta \sin(\omega t)]$$

and

$$\begin{aligned} \dot{U}_N &= a \equiv -\frac{\pi R_N^2}{M} \left(\frac{\hat{\mu}_N}{L} \frac{U_N - U_{N-1}}{h} + \frac{\sigma}{R_N} \right), \\ \dot{L} &= U_N. \end{aligned}$$

Time integration and initial conditions

The semi-discretisation using finite difference approximation results in a system of (non-linear) ordinary differential equations which is solved using a standard built-in Matlab time integrator `ode23s`, starting from $t = t_0$. The initial values of the tail length L_0 is assumed to be an arbitrary small value. The velocity for the tail and the droplet $u(x, t_0) = V(t_0)$ and the radius of the droplet R_s can be calculated once we know t_0 , the time when the droplet forms.

The value of t_0 is the non-trivial solution of the following equation

$$T_{k.e.} = T_{k.e.l} + T_{s.e.l} \quad (1)$$

which can be solved using Maple.

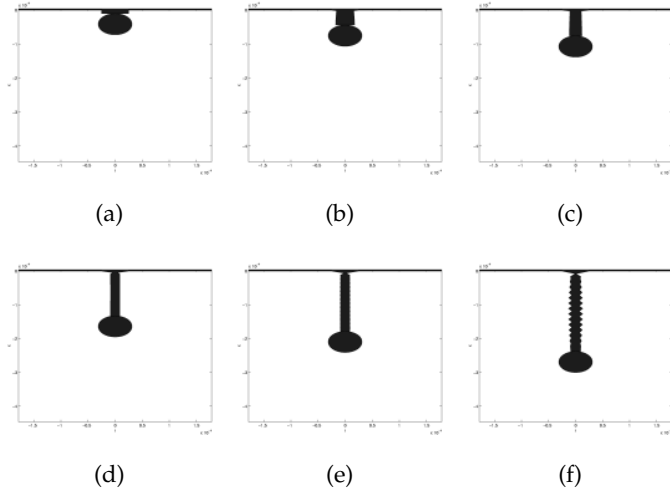


Figure 5 Case 4. Visco-elastic fluid with $k = 10^{-5}$. Shape of the tail at (a) $t = 0$; (b) $t = 0.5t_0$; (c) $t = t_0$; (d) $t = 2t_0$; (e) $t = 3t_0$; (f) $t = 5t_0$.

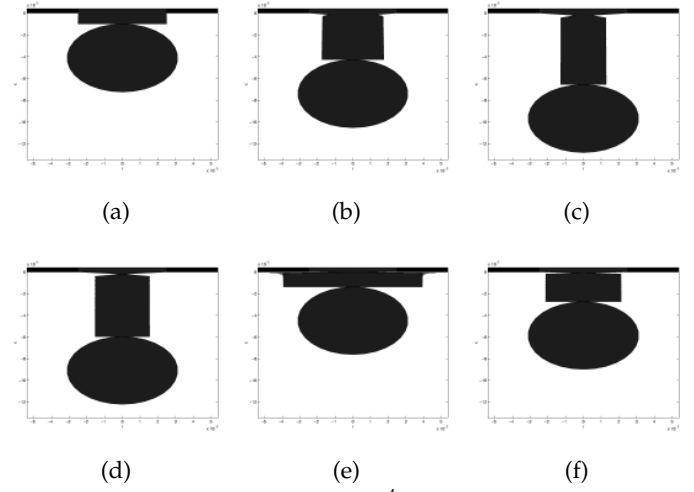


Figure 6 Case 5. Visco-elastic fluid with $k = 10^{-4}$. Shape of the tail at (a) $t = 0$; (b) $t = 0.5t_0$; (c) $t = t_0$; (d) $t = 2t_0$; (e) $t = 3t_0$; (f) $t = 5t_0$.

Results

The parameter values for the numerical simulations are: $V_n = 5 \text{ m} \cdot \text{s}^{-1}$, $\omega = 4\pi \times 10^4 \text{ s}^{-1}$, $R_n = 2.5 \times 10^{-5} \text{ m}$, $\rho = 10^3 \text{ kg} \cdot \text{m}^{-3}$, and $\sigma = 3 \times 10^{-2} \text{ N} \cdot \text{m}^{-1}$. We have used a power-law model for the elongational viscosity $\hat{\mu}$ based on the experimental data in [2]

$$\hat{\mu} = \begin{cases} 3 \times 10^{-3}, & |\dot{\epsilon}| \leq 10^3 \text{ s}^{-1} \\ 3 \times 10^{-3} \left(\frac{|\dot{\epsilon}|}{10^3} \right)^\gamma, & \text{otherwise} \end{cases}$$

in Pascal. Here $\dot{\epsilon} = u_x$ is the axial strain-rate, γ is a free parameter and for Newtonian fluid, $\gamma = 0$. Other free parameters are the elastic constant k , initial tail length L_0 , and tail radius near the nozzle exit R_c .

Initial and boundary conditions

The initial conditions are computed based on t_0 , the time when the droplet forms, which is estimated based on energy arguments. With the velocity profile at the nozzle exit V without any damping ($\beta = 0$), equation (1) becomes

$$2 \cos^2 \omega t_0 - \cos \omega t_0 - \frac{6\sigma C}{\rho A V_n^2} = 1$$

where $C = 2\pi R_n$ is the circumference of the liquid cylinder. Based on the parameter values given here, the non-trivial solution can be obtained using Maple as $\omega t_0 = 2.308$. The total volume of the droplet and the tail can be computed as

$$\text{Vol} = \int_0^{t_0} A_n V dt = \frac{A_n V_n}{\omega} (1 - \cos \omega t_0) = 1.306 \times 10^{-13}$$

in m^3 . In our computation, we assume that a certain portion of it forms the spherical droplet and the rest becomes the tail. Thus we should have the following constraint on the droplet radius

$$R_s \leq \left(\frac{3\text{Vol}}{4\pi} \right)^{\frac{1}{3}} = 3.148 \times 10^{-5}$$

in m . The initial velocity of the droplet and the tail is assumed to be equal to that near the nozzle exit with radius R_c , which is

$$U_j(0) = V_c(0) \equiv \frac{R_n^2}{R_c^2} V_n \sin(\omega t_0) = 3.702 \frac{R_n^2}{R_c^2}$$

in $\text{m} \cdot \text{s}^{-1}$. Therefore, it depends on the radius of the initial tail radius $R_c \leq R_n$, which is chosen as a free parameter here. The initial length of the tail L_0 , can in principle be estimated based on the choice of R_s and R_c . However, its value is chosen as a small but non-zero value 10^{-5} m for computational purposes. Finally, the boundary condition for velocity is given by

$$U_0(t) = V_c(t) \equiv \frac{R_n^2}{R_c^2} V = \frac{R_s^2}{R_c^2} V_n \sin(\omega t).$$

Power-law non-Newtonian fluid

We now present some of the computational results based on the model and the parameter values listed earlier with no elastic effect, i.e., $k = 0$. In figure 2, the evolution of the droplet tail is shown for $R_s = 1.25R_n$, $R_c = R_n$, and $V_c = V$. We have also included damping in V with the damping rate $\beta = \frac{\log(2)}{2} \omega$. The non-Newtonian power-law parameter is chosen as $\gamma = 1.1$. Figure 3 shows the tail evolution for the case when the radius of the tail near nozzle exit is reduced to half of the nozzle radius, i.e. $R_c = 0.5R_n$. This causes the tail to break up sooner, compared to the previous case with a large R_c . Next we have investigated the effect of parameter γ . In figure 4, we have the same parameter values as in case 1, except that $\gamma = 1.5$. It can be seen that the larger value of γ delays the breakup of the tail. Note that this case corresponds to higher molecular weight polymer solutions.

Visco-elastic fluid

The visco-elastic effect of the fluid on the tail is investigated numerically by giving non-zero values to the spring constant k and the results are presented in figures 5 and 6. It can be seen from the figures that the elasticity has visible effects. For the small spring constant case ($k = 10^{-5}$), the 'satellite' droplets appear but it is not clear whether this is physical or due to numerical instability. For the large k case, the elasticity is dominant and the droplet has been pulled back toward the nozzle exit and the tail acts as a spring.

Conclusion

We have presented a one-dimensional model to predict the breakup of the liquid filament (tail) attached to an ink-jet droplet. The effect of a power-law non-Newtonian stress-strain relationship on the evolution of the tail is investigated by solving the model equations numerically. The results clearly show the delay (and sometimes lack) of breakup of the droplet tail for higher power relationships. This is consistent with the experimental evidence for higher molecular weight polymer solutions. The elasticity effect on the behaviour of the tail was also investigated. However, it is not clear whether the appearance of 'beads' on the tail, resembling those satellite droplets observed experimentally, are physical or due to numerical instability.

The numerical results also suggest that the mechanism for the breakup of the tail is most likely not surface tension driven since the viscous stress is much bigger than the surface tension based on the calculation. The oscillatory nature of the pump drives the flow at the nozzle exit and reverses its direction periodically. As a result, the flow inside the liquid filament (tail) near the exit may be 'sucked' back while the rest of the tail still moves forward with the main droplet. This causes a decrease of fluid mass locally near where the flow velocity changes direction and forms a 'neck'. Surface tension may become a contributing factor after the formation of the neck and speed up the breakup process. It is possible that a theoretical model can be developed to predict the final breakup using a similarity solution. However, this is not pursued in the current study.

In summary, these simulation results seem to suggest that the one-dimensional model captures the essential features of the breakup of ink-jet droplet tails. A positive connection between

the length of the tail and molecular weight is established from the fact that delays in breakups usually result in a longer tail. And the delay can be attributed to the higher power in the power-law elongational viscosity, which is one of the consequences of higher molecular weight in the polymer solution. However, it must be noted that the current model has its limitations. First of all, we have ignored the dynamical evolution of the droplet and the flow between the tail and the droplet. Secondly, the flow near the exit is certainly not one-dimensional. Contrary to Newtonian flows where the exit liquid jets contract, the visco-elastic jets increase their diameters ('die swell') after the exit [3]. Therefore, a more careful study is needed to capture all the dynamics correctly and two or higher dimensional models will be needed. ◀

Acknowledgments

The report is based on the discussions among the participants who worked on the problem during the workshop, and helpful comments by P. Duineveld and by P. Howell from Oxford. Numerical results were obtained by J.F. Williams during the workshop and are re-produced by the author.

Participants

Participants who worked on this problem are: Frits Dijkman (Philips Research), Paul Duineveld (Philips Research), Fieke Dekkers (Utrecht), Johan Dubbeldam (Eindhoven), Yodi Gunawan (Eindhoven), Huaxiong Huang (York), Simon Kronemeijer (Amsterdam), Mikhail Tchesnokov (Eindhoven), Jan Bouwe van den Berg (Nottingham), Rein van de Hout (Leiden), J.F. Williams (Bath).

Notes and references

- 1 The set of equations are based on the assumption that the problem is one-dimensional. It can also be derived formally using asymptotic argument, similar to the procedure outlined in [6].
- 2 M. Stelter, G. Brenn, A.L. Yarin, R.P. Singh and D. Durst, Investigation of the elongational behaviour of polymer solutions by means of an elongational rheometer, *J. Rheol.* **46**(2), 507–527 (2002).
- 3 R.B. Bird, R.C. Armstrong and O. Hassager, *Dynamics of Polymeric Liquids*. John Wiley & Sons, NY (1987).
- 4 D.W. Bousfield et al., Nonlinear analysis of the surface tension driven breakup of visco-elastic filaments, *J. Non-Newt. Fluid Mech.* **21**: 79–97 (1985).
- 5 J.F. Dijkman, Hydro-acoustics of piezoelectrically driven ink-jet print heads, *Turbulence and Combustion* **61**: 211–237 (1999).
- 6 A.D. Fitt et al, Modeling the fabrication of hollow fibers: capillary drawing, *J. Lightwave Tech.* **19**(12): 1924–1931 (2001).
- 7 J. Eggers, Theory of drop formation, *Phys. Fluids*. **7**: 941–953 (1995).
- 8 D.T. Papageorgiou, On the breakup of viscous liquid threads, *Phys. Fluids* **7**: 1529–1544 (1995).
- 9 M. Renardy, Some comments on the surface-tension driven break-up (or the lack of it) of visco-elastics jets, *J. Non-Newt. Fluid Mech.* **51**: 97–105 (1994).
- 10 M. Renardy, A numerical study of the asymptotic evolution and breakup of Newtonian and visco-elastic jets, *J. Non-Newt. Fluid Mech.* **59**: 267–282 (1995).
- 11 M. Stelter et al, Investigation of elongational behaviour of polymer solutions by means of an elongational rheometer, *J. Rheol.* **46**(2): 507–527 (2002).
- 12 A.L. Yarin, *Free Liquid Jets and Films: Hydrodynamics and Rheology*, Longman, Harlow (1993).